JOURNAL OF GEOPHYSICAL RESEARCH, VOL. 111, A12317, doi:10.1029/2006JA011679, 2006

A total electron content space weather study of the nighttime Weddell Sea Anomaly of 1996/1997 southern summer with TOPEX/Poseidon radar altimetry

Ildiko Horvath[1]

Received 19 February 2006; revised 5 September 2006; accepted 21 September 2006; published 23 December 2006.

[1] This paper reports on a total electron content space weather study of the nighttime Weddell Sea Anomaly, overlooked by previously published TOPEX/Poseidon climate studies, and of the nighttime ionosphere during the 1996/1997 southern summer. To ascertain the morphology of spatial TEC distribution over the oceans in terms of hourly, geomagnetic, longitudinal and summer-winter variations, the TOPEX TEC, magnetic, and published neutral wind velocity data are utilized. To understand the underlying physical processes, the TEC results are combined with inclination and declination data plus global magnetic field-line maps. To investigate spatial and temporal TEC variations, geographic/magnetic latitudes and local times are computed. As results show, the nighttime Weddell Sea Anomaly is a large ($\sim$1,600($^\circ$)^2; $\sim$22 million km^2 estimated for a steady ionosphere) space weather feature. Extending between 200°E and 300°E (geographic), it is an ionization enhancement peaking at 50°S–60°S/250°E–270°E and continuing beyond 66°S. It develops where the spacing between the magnetic field lines is wide/medium, easterly declination is large-medium (20°–50°), and inclination is optimum ($\sim$55°S). Its development and hourly variations are closely correlated with wind speed variations. There is a noticeable ($\sim$43%) reduction in its average area during the high magnetic activity period investigated. Southern summer nighttime TECs follow closely the variations of declination and field-line configuration and therefore introduce a longitudinal division of four (Indian, western/eastern Pacific, Atlantic). Northern winter nighttime TECs measured over a limited area are rather uniform longitudinally because of the small declination variation. TOPEX maps depict the expected strong asymmetry in TEC distribution about the magnetic dip equator.

Citation: Horvath, I. (2006), A total electron content space weather study of the nighttime Weddell Sea Anomaly of 1996/1997 southern summer with TOPEX/Poseidon radar altimetry, *J. Geophys. Res.*, *111*, A12317, doi:10.1029/2006JA011679.

1. Introduction

[2] The concept of TOPEX/Poseidon mission was born in the early 1980s when NASA JPL (National Aeronautics and Space Administration Jet Propulsion Laboratory) and CNES (Centre National d'Etudes Spatiales) joint their separate research plans, TOPEX and Poseidon, respectively, to form one single mission. Its main objective was the study of large-scale oceanic circulations and their interaction with the atmosphere to better understand the climatic changes. Originally, the Ocean Topography Experiment (TOPEX) was designed to measure the sea level height of the world oceans with an altimeter. Meanwhile, the Poseidon project, named for the Greek god of sea, was planned to be a scientific oceanographic assignment [*Fu et al.*, 1994; *Menard et al.*, 1995; *Jee et al.*, 2004]. The joint TOPEX/Poseidon mission started in August 1992 and continued through a 3-year prime mission and an extended observational phase. Since the satellite is still producing high-quality data, NASA decided to continue the operation through 2003 and beyond [*Jee et al.*, 2004].

[3] The TOPEX/Poseidon mission is the first very ambitious satellite radar altimetry mission in terms of performances. It is equipped with a Ku-band (f_{Ku} = 13.6 GHz) and C-band (f_C = 5.3 GHz) frequency NASA Radar Altimeter (NRA) of which main objective is to measure sea level heights at the vertical of the satellite, every 6 km or 1 s in time with an accuracy of 13 cm [*Fu et al.*, 1994; *Menard et al.*, 1995]. To provide such accuracy, both the position of the satellite and any propagation path delays between the sea surface and the satellite must be known accurately. Owing to the large number of free electrons, there are changes in the atmospheric refractive index. As a result, radar pulses travelling through the ionosphere on their way between the satellite and the sea surface become delayed leading to errors that can exceed 25 cm in height measurements [*Codrescu et al.*, 2001]. Ionospheric time delays can be estimated to first order by transmitting at two frequencies

[1]Electromagnetics and Imaging, School of Information Technology and Electronic Engineering, University of Queensland, Brisbane, Queensland, Australia.

0148-0227/06/2006JA011679$09.00

[*Monaldo*, 1993; *Robinson and Beard*, 1995]. Through the use of NRA, a fairly high accuracy is achievable. Usually, the path delay errors are less than 3 cm [*Codrescu et al.*, 1999]. By overreaching largely the initial objective of 13 cm accuracy, it was soon realized that the TOPEX/Poseidon system marked a new era in altimetry.

[4] By performing a simple linear transformation, the total electron content or TEC can be obtained from the ionospheric time delays. TEC provides an overall description of the ionization of the ionosphere and is a key parameter for various space weather applications. Since the onset of TOPEX/Poseidon mission, more than 10 years of ionospheric height correction data became available that are feasible for obtaining an equally large TOPEX TEC database for investigating TEC climatology over the oceans. Completed in two phases, *Codrescu et al.* [1999, 2001] created a customized TOPEX TEC database representative of low-solar activity (F10.7 < 120) as it covers the solar minimum between solar cycles 22 and 23 and utilized this database to map global TEC patterns in magnetic local time (MLT) versus magnetic latitude (MLAT) coordinates. Averaged TEC values were obtained by binning the data into 1°MLAT by 1°MLT cells. During the first phase of research, measurements from almost 5 years extending from the launch of the satellite (1992) to 1996 had been gathered in order to analyze the average spatial structure of the ionosphere and to investigate global TEC climatology and storm time TEC signatures of the middle- and low-latitude ionosphere [*Codrescu et al.*, 1999]. This original database had been updated through 1997 during the second phase of research. Containing experimental TOPEX and DORIS TEC measurements plus empirical IRI and Bent model results, a complete database that is particularly suitable for model validation purposes had been created [*Codrescu et al.*, 2001]. In order to study TEC climatology that is inherent in the TOPEX data and to compare low solar activity (F10.7 < 120) results with the findings of *Codrescu et al.* [1999], *Jee et al.* [2004] also binned the TOPEX data from 1992 to 2001 according to the F10.7 cm flux value of 120, and according to the averaged Kp values of 1.0, 2.5 and 4.2 denoting low, medium, and high geomagnetic activities, respectively. TEC climatology was studied during the seasons of equinoxes and solstices over the oceans that naturally divide the ionosphere into the longitude sectors of Pacific, Atlantic, and Indian. For general climatology study, MLT versus MLAT maps were constructed by binning the data into 1°MLAT by 1°MLT cells. For longitudinal and seasonal TEC studies, the map's cell size was increased to 15°MLAT by 1°MLT and to 2°MLAT by 3.75°MLT, respectively. *Jee et al.* [2005a] also performed a comprehensive comparison of TOPEX TEC measurements with the up to date version of the International Reference Ionosphere (IRI-2001). The binning resolution of MLAT versus MLT maps remained 2° by 3.73°. In both studies of *Jee et al.* [2004, 2005a], the unusually high nighttime TEC values at high geographic latitudes during equinoxes (F10.7 > 120) and summer solstices (F10.7 $\geq$ 120 and F10.7 < 120), peaking at around 250°E geographic longitude, were noticed but were not related to the nighttime phenomenon of the Weddell Sea Anomaly. Because the data binning procedure (applied in the above-mentioned TEC climatology studies) smears the longitude dependent features, none of the global TOPEX TEC maps constructed for equinoxes and summer solstices shows the image of neither the daytime Weddell Sea Anomaly nor the nighttime Weddell Sea Anomaly.

[5] In the southern ionosphere during winter and equinoxes/summer solstices, two prominent large-scale ionospheric space weather features, commonly called the Weddell Sea Anomaly by *Penndorft* [1965], dominate space weather. These are the daytime and the nighttime phenomenon of the Weddell Sea Anomaly, respectively. They develop over the same geographic area, which extends across the southeastern Pacific and southwestern Atlantic Oceans [*Horvath and Essex*, 2003]. Their development can be explained by the unusual combination of solar produced ionization (abundant at summer nights and limited at winter days due to the tilted geomagnetic field) and thermospheric neutral winds (equatorward directed during the night and poleward directed at daytime) in the Antarctic region where the distance between the geomagnetic and geographic poles is twice as large as that in the northern hemisphere [*Clilverd et al.*, 1991, and references therein]. The daytime Weddell Sea Anomaly is an unusually large electron density depletion that reaches its best developed form at around 1400 LT. The nighttime Weddell Sea Anomaly appears as a substantial electron density increase peaking between 2200 LT and local midnight. In the Weddell Sea Anomaly region, the ionosphere shows a typical magnetic midlatitude behavior during early equinoxes when the electron density peaks at daytime and the minimum occurs at nighttime. Following this usual period and occurring on a sequence of days during equinoxes, this typical behavior becomes changed by a sudden switch that is also part of the peculiar F2 region behavior that *Penndorft* [1965] commonly called the Weddell Sea Anomaly.

[6] *Horvath and Essex* [2003] detected just about the complete image of both phenomena during the 1998/1999 high-sunspot summer period by utilizing the TOPEX/Poseidon technique. They pointed out first that the real size of the Weddell Sea Anomaly is much larger than was thought previously by other researchers based upon their land-based ionosonde observations at Faraday, the name of the ionosonde station at Argentine Islands (295.7°E; −65.3°N, geographic) that is now called Vernadsky, in Antarctica providing only a limited data coverage [*Bellchambers and Piggott*, 1958; *Penndorft*, 1965; *Dudeney and Piggott*, 1978; *Clilverd et al.*, 1991]. With a series of TOPEX TEC maps, *Horvath and Essex* [2003] demonstrated that larger part of the Weddell Sea Anomaly is situated west of Argentine Islands over the Bellingshausen Sea, not over the Weddell Sea that is east of Argentine Islands, and concluded that it should be called the Bellingshausen Sea Anomaly.

[7] The main goal of this paper is to investigate in detail the TEC variation of the nighttime Weddell Sea Anomaly and to study the nighttime TEC space weather over the oceans during the low sunspot number 1996/1997 southern summer solstice between 28 November 1996 and 5 February 1997. TOPEX/Poseidon radar altimetry is used to obtain ionospheric TEC values and to observe space weather over the oceans. TOPEX TEC maps are constructed with the data obtained from the nighttime cycles and individual TOPEX TEC passes provide latitudinal TEC cross sections sometimes along the magnetic field lines. Longitudinal TEC cross sections that cross the magnetic field lines along

various middle geographic latitudes are prepared. Observational results presented in the above mentioned manner are analyzed in this paper to ascertain the morphology of the spatial TEC distribution over the oceans. Because the thermospheric neutral winds have a major role in creating and maintaining the unusually high nighttime TEC of the Weddell Sea Anomaly, the configuration of magnetic field lines is mapped not only with the ground tracks of individual TOPEX passes but over the TEC maps as well. Further, the magnetic declination and inclination data are also utilized for the TOPEX TEC analysis to highlight the role of equatorward directed neutral winds. To introduce a custom-made software package developed for obtaining TOPEX TEC values and for constructing TEC line plots and maps from the NRA ionospheric height corrections is another main aim of this paper.

2. TOPEX TEC Theory

[8] Operating at nadir direction only, the dual-frequency Ku/C band (f_{Ku} = 13.6 GHz; f_C = 5.3 GHz) NASA radar altimeter generates a radar pulse at each frequency to measure their return distances from the surface of the ocean. Each radar pulse experiences a time delay because of the enlarging effects of ionized medium as it travels through the ionosphere. At the two operating frequencies, the two one-way time delays (ΔT_1 and ΔT_2; in nanoseconds) can be computed in a first-order approximation according to equations (1) and (2) [*Monaldo*, 1993]. These positive differential time delay values indicate that the ionosphere lengthens the electromagnetic path of each signal.

$$\Delta T_1 = \frac{A}{c f_{Ku}^2} \int_R^S N ds \tag{1}$$

and

$$\Delta T_2 = \frac{A}{c f_C^2} \int_R^S N ds \tag{2}$$

A = constant = 40.31 (m^3/s^2),
c = speed of light,
f_{Ku} = Ku-band operating frequency (defined above),
f_C = C-band operating frequency (defined above),
S = satellite altitude = 1336 km,
R = sub-satellite reflection point,
N = electron density (e/m^3),
ds = element of ray path (m)

[9] Differential time delay ($\Delta\delta T$; in nanoseconds) is the difference between the two one-way time delay measurements and is linearly proportional to the integral of electron density:

$$\delta\Delta T = \Delta T_2 - \Delta T_1 = \frac{A}{c}\left(\frac{1}{f_C^2} - \frac{1}{f_{Ku}^2}\right)\int_R^S N ds$$
$$= \left(\frac{f_{Ku}^2 - f_C^2}{f_C^2}\right)\frac{A}{c f_{Ku}^2}\int_R^S N ds \tag{3}$$

An absolute path difference (in mm) between the two one-way signals can be computed as:

$$\delta\Delta P' = \delta\Delta T * c = \left(\frac{f_{Ku}^2 - f_C^2}{f_C^2}\right)\frac{A}{f_{Ku}^2}\int_R^S N ds \tag{4}$$

By substituting the appropriate frequencies and the constant value of A in, an ionospheric height correction (in mm) can be obtained as:

$$\delta\Delta P' = -\frac{403.1}{f_{Ku}^2}\int_R^S N ds \tag{5}$$

$\int_R^S N ds$= vertical total electron content or TOPEX TEC (in TECU), 1 TECU = $10^{16} \frac{e^-}{m^2}$.

[10] The negative sign indicates that this extra length correction ($\delta\Delta P'$), which is an ionospheric error in the height measurement, has to be taken away from the combined measured height in order to obtain a true geometric height [*Monaldo*, 1993].

3. Software

[11] A tailor-made software package, made up of several computer programs, was developed to utilize the ionospheric height correction ($\delta\Delta P'$ in mm) for obtaining vertical TEC or TOPEX TEC, which is equivalent with the integral of electron density (N) between the satellite (S) orbiting at 1336 km height and the subsatellite reflection point (R) on the surface of the ocean (see equation (6)).

$$\text{TOPEX TEC} = \int_R^S N ds = -\frac{f_{Ku}^2}{403.1}\delta\Delta P' \tag{6}$$

For each TOPEX TEC value, the local time was also computed. Further, the TOPEX TEC values had to be averaged out as the altimeter data are affected by varying noise due to wave height variations (see red curve in Figure 1). A 20-s time or ~1° latitude interval [*Codrescu et al.*, 2001], which is equivalent with a 116 km spatial distance, was found reasonable to smooth the TEC curve (see green curve in Figure 1) and also to maintain the data accuracy at the same time. Finally, by binning the smoothed TEC data of odd or even passes into 2° latitude by 4° longitude cells, averaged TEC values were obtained for the construction of TOPEX TEC maps.

4. Experimental Considerations

[12] Satellite of the TOPEX/Poseidon mission travels with an orbital velocity of 7.2 km/s, while the ground track speed is 5.8 km/s, and covers the Earth (see Figure 2) in a close to 10-day (9.916-day) repeat cycle (available at ftp://podaac.jpl.nasa.gov/pub/sea_surface_height/topex_poseidon/mgdrb/doc) [*Jee et al.*, 2004]. A complete repeat cycle is made up of 254 passes. For convenience, cycles and passes are designated by numbers. Figure 2 shows the ground tracks of all the 254 passes plotted in the grid

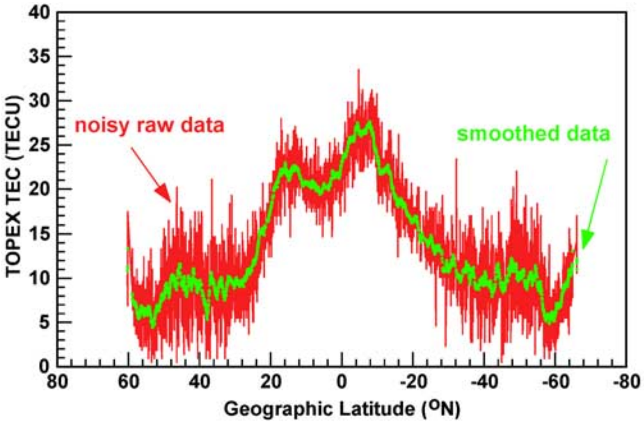

Figure 1. Two line plots created for a TOPEX pass show the raw (indicated in red) and smoothed (indicated in green) TOPEX total electron content (TEC) curves in geographic latitudes. The raw data curve shows a varying noise effect due to the irregular height variations of ocean waves.

of geographic parallels. As the altimeter data are not processed over the continents, there is data coverage over the oceans only. An Earth orbit is made up of two passes. An example of an Earth orbit is illustrated with passes 41 and 42 (indicated in yellow) in Figure 3 where the local time (LT) and universal time (UT) in decimal hours are also stated at the start and end of each pass. The TOPEX/Poseidon satellite's orbital period is 112 min or 1.87 hours in UT. Because of the 66° inclined orbit, a satellite orbit crosses over two hemispheres between ±66°N geographic latitude degrees (see Figure 3). Altogether, there are 127 even-numbered, descending or southbound passes and 127 odd-numbered, ascending or northbound passes. In Figure 3 the ground tracks of some of the even- and odd-numbered passes are plotted with the magnetic field lines to show the alignment of TOPEX passes with respect to the field-line configuration. Over the Pacific Ocean the odd-numbered passes at some extent are aligned with the magnetic field lines (example 41, 43, 45, and 47; see Figure 3), while the even-numbered passes follow the field-line trends at low latitudes over the Atlantic Ocean (example 48; see Figure 3) and at midlatitudes over the Indian Ocean (example 46, 44, and 42 from left to right; see Figure 3). Passes can be characterized by their equator crossing longitudes EQ(Lon). At the geographic equator, two consecutive passes are situated 166° (geographic longitude) apart and two adjacent passes are separated by 28°. In UT, 0.935 Hr is the traveling time of any pass, during which the local time changes greatly as the TOPEX pass crosses many geographic longitudes, whilst the universal time remains similar (see UT and LT values of passes 41 and 42 in Figure 3).

5. TOPEX TEC Data

[13] The TOPEX TEC data presented in this paper cover the low sunspot number period of 28 November 1996 to 5 February 1997, inclusive, situated at the bottom of the ascending phase of solar cycle 23 where the F10.7 cm flux is around 90.

[14] By plotting the smoothed TEC data from the passes against the geomagnetic latitudes, the TOPEX TEC line plots are constructed. Owing to the short UT spans (0.935 hour) of passes, the TOPEX line plots are like snapshots that image the ionosphere in latitudes across two hemispheres in case of continuous data coverage. For analyzing purposes, both the local time (LT defined with respect to the Sun and geographic pole) and the magnetic local time (MLT defined with respect to the Sun and geomagnetic pole) are utilized.

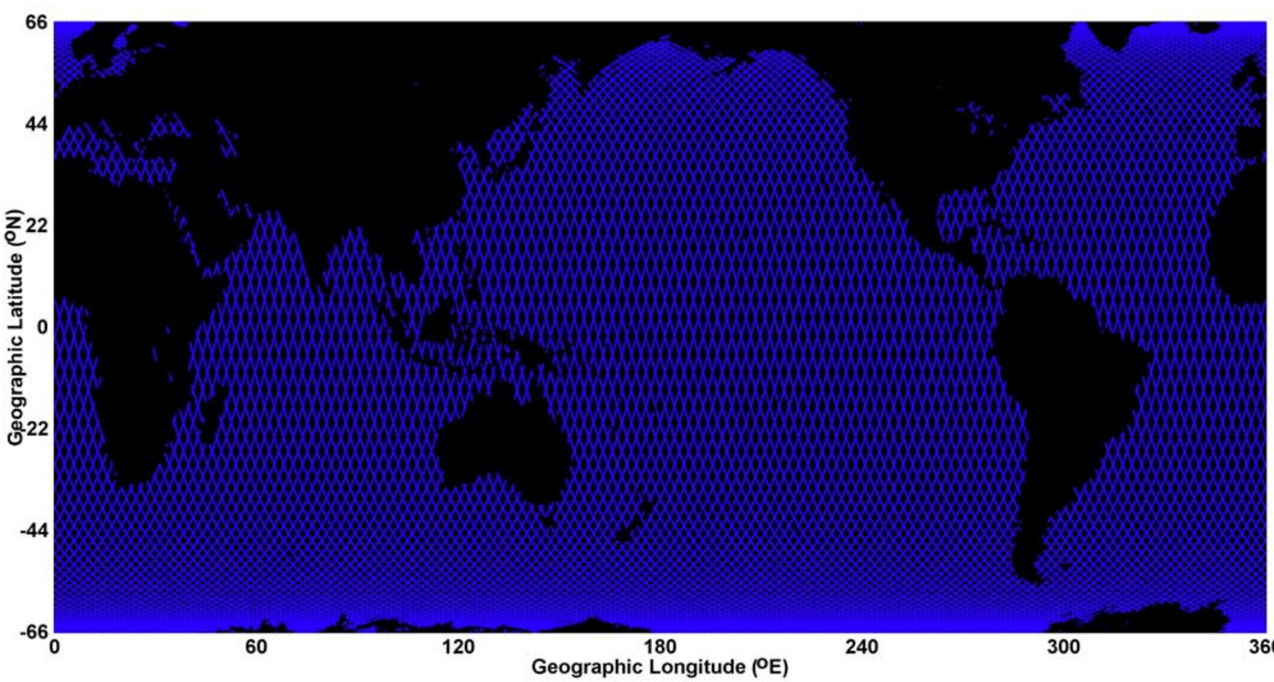

Figure 2. In the form of a global map the ground tracks of TOPEX/Poseidon satellite are plotted for cycle 155 (28 November to 8 December 1996) in the grid of geographic parallels.

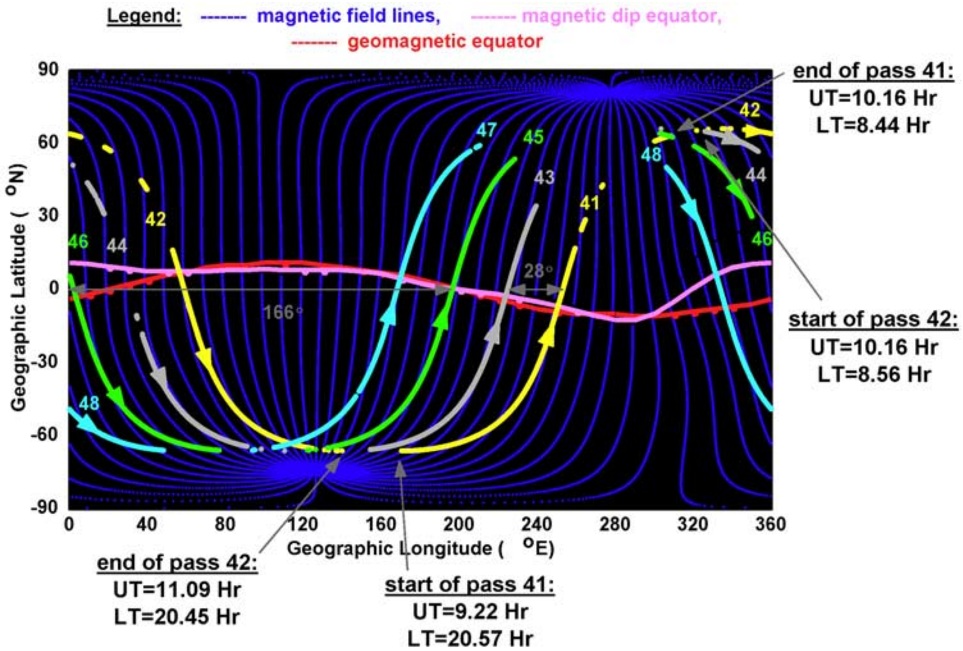

Figure 3. Some odd-numbered or ascending passes and even-numbered or descending passes are plotted with the magnetic field lines (indicated in dark blue) and with the geomagnetic (indicated in red) and magnetic dip (indicated in pink) equators. To illustrate the variations of universal time and local time during an Earth orbit composed by an odd- and an even-numbered pass (indicated in yellow), UT and LT values of passes 41 and 42 are stated. The arrows indicate the TOPEX/Poseidon travelling direction.

For each 24 hour LT day, MLT advances also by 24 hours but not at a uniform rate [*Rishbeth*, 1986]. Therefore it is important to monitor both the LT and the MLT variations in latitudes. Owing to the alignment of ground tracks, there is a 3-hour LT variation between 60 and 66 geographic latitudes and only a 2-hour LT variation between 40°N and 40°S. In a more irregular manner, MLT also exhibits great variations in geomagnetic latitudes (see details in section 6.1). As both LT and MLT vary greatly, over 8 hours, with latitudes because of the large ground coverage of the passes, the TEC line plots are not snapshots in terms of LT and MLT.

[15] Altogether, seven cycles are mapped from 155 to 161, inclusive, by binning the smoothed data into 2 latitude degree × 4 longitude degree (geographic) cells and by plotting the binned TEC values in the grid of geographic parallels. With the exception of cycle 155, where all the even-numbered passes are considered, each TOPEX TEC map is created by utilizing all the available (up to 127) odd-numbered passes as those passes cover the local nighttime sector of the relevant 10-day cycle. TOPEX TEC maps have large latitudinal local time variations across all longitudes. Owing to these large latitudinal local time variations across all longitudes, these maps contain both spatial and temporal variations. In order to keep track on larger-scale local time variations, each map also indicates the geographic equator crossing local time (EQ(LT)) and the local time at the highest latitude of the Weddell Sea Anomaly (WSA(LT)). During any cycle, there is an approximately 2 hour LT difference between the first and last pass crossing the equator. For sake of simplicity, the EQ(LT) stated at each map indicates a median value (i.e., the equator crossing local time of pass number 127 (in case of an odd-numbered cycle) or of pass number 128 (in case of an even-numbered cycle)). Precisely, the local time covered at the equator is EQ(LT) ± 56 min, approximately it is EQ(LT) ± 1 hour. Similarly, the local time changes at Weddell Sea Anomaly latitudes. In this study, an approximate EQ(LT) and WSA(LT) are indicated for each map. Because of these large spatial and temporal variations introduced by the 10-day data utilized, these maps are not snapshots from space. In each hemisphere these maps depict a realistic nighttime ionosphere only if the ionosphere did not change significantly (i.e., remained almost steady) during those local times hours. This steady ionosphere assumption was assumed when the geographic area of nighttime Weddell Sea Anomaly was estimated for comparative reasons only.

[16] To study the magnetic alignment of space weather features detected in the data, the geomagnetic (indicated in red) and magnetic dip (indicated in pink) equators are plotted over each TEC map. To observe the underlying geophysical activity, the most widely used 3-hour Kp index is plotted for each cycle mapped and an average Kp value is computed for the period of each cycle (see Figure 4).

6. TEC Space Weather Observations and Discussions

6.1. Hourly Variations of the Nighttime Weddell Sea Anomaly

[17] To study the hourly variations of the nighttime Weddell Sea Anomaly during the 1996/1997 southern summer, seven nighttime TOPEX TEC maps are prepared imaging it in every 2 hours from 1600 LT (median value) to 0250 LT, inclusive. During the seven TOPEX cycles mapped, the average local time at the equator changes also by two

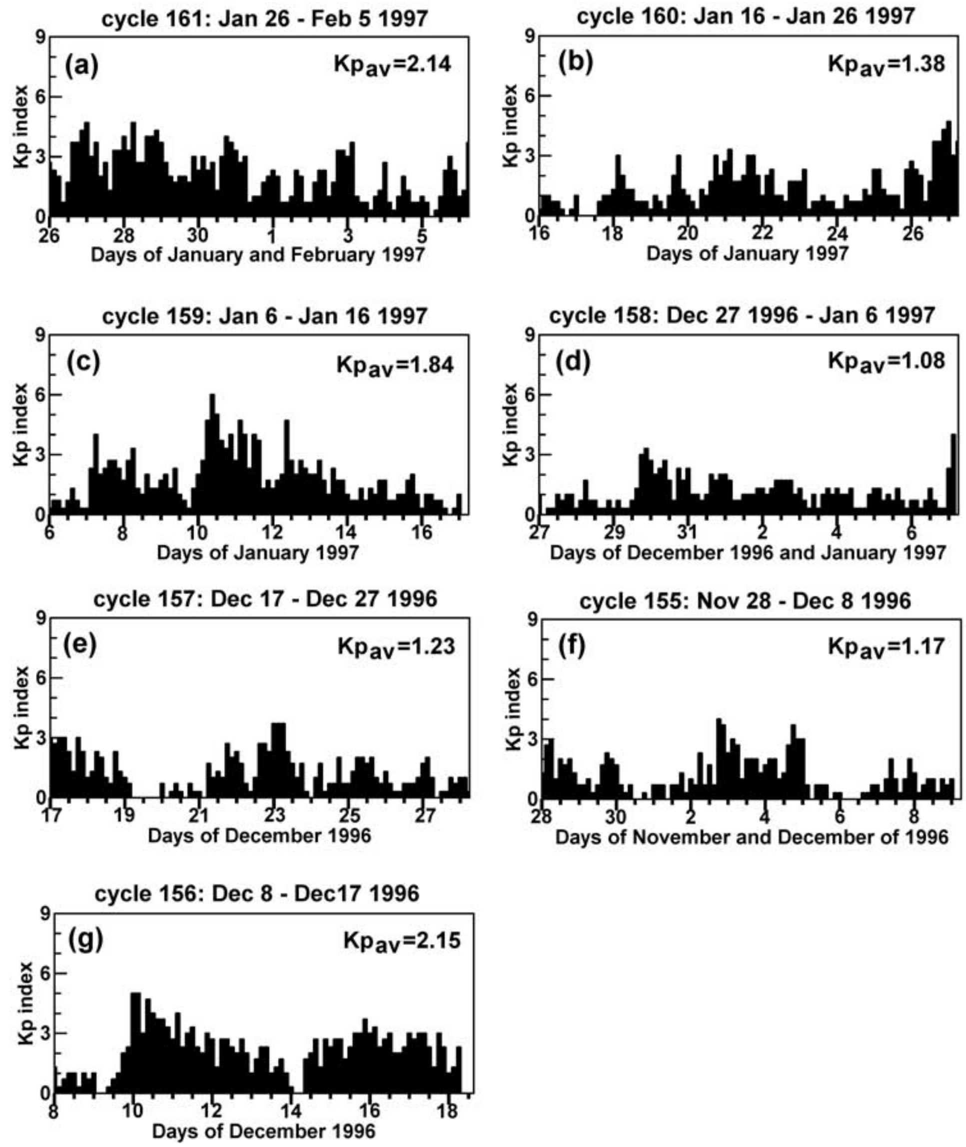

Figure 4. A series of Kp histograms, prepared for the TOPEX cycles mapped, shows the variations of geophysical conditions during the cycles. These histograms are arranged in the same order as the TOPEX TEC maps. An averaged Kp value is also indicated for each cycle.

hours from 2200 LT (cycle 161) to 0800 LT (cycle 156), inclusive. For simplicity, LT values at the geographic equator (indicated as EQ(LT)) and at the Weddell Sea Anomaly (indicated as WSA(LT)) are discussed. Logically, these maps in Figure 5 are arranged according to the local time values at the Weddell Sea Anomaly (WSA(LT)) in an increasing order. All the maps showing the Weddell Sea Anomaly suggest that it continues at latitudes higher than 66°S (geographic) where there is no data coverage because of the 66° inclined satellite orbit. In order to get an indication of the size of the Weddell Sea Anomaly, its area is estimated in latitude by longitude degrees or $(°)^2$ and in million (10^6) km^2 from the TEC maps by considering TEC values higher than 18 TECU (indicated in light and dark pink). These estimated values are realistic only under the assumption that the appearance of the nighttime Weddell Sea Anomaly changed little during the approximately 4-hour LT variation taking place across it (i.e., between its northern top and the 66°S latitude). For comparative reasons only, the estimated areas are utilized to quantify the nighttime variation of the Weddell Sea Anomaly during the studied period.

[18] In the first map (i.e., cycle 161; see Figure 5a) the most prominent feature is a large evening (∼1800–2000 LT) electron density buildup over the Southern Pacific and South-Western Atlantic Oceans. Because of the early local time (1600 LT) at high latitudes, the Weddell Sea Anomaly had not formed yet. At around 60°S and higher geographic latitudes, the TEC is lower (17 TECU indicated in dark blue) than at southern midlatitudes where the TEC reaches its maximum (18–20 TECU indicated in light pink). On the next four maps (see Figures 5b–5e), the Weddell Sea Anomaly becomes the most prominent space weather feature (18–20 TECU and 20+ TECU indicated in light and dark pink) from 1800 LT to 2400 LT (i.e., WSA(LT)). Its development starts at about 1700 LT when the thermospheric neutral winds in the magnetic meridional direction turn

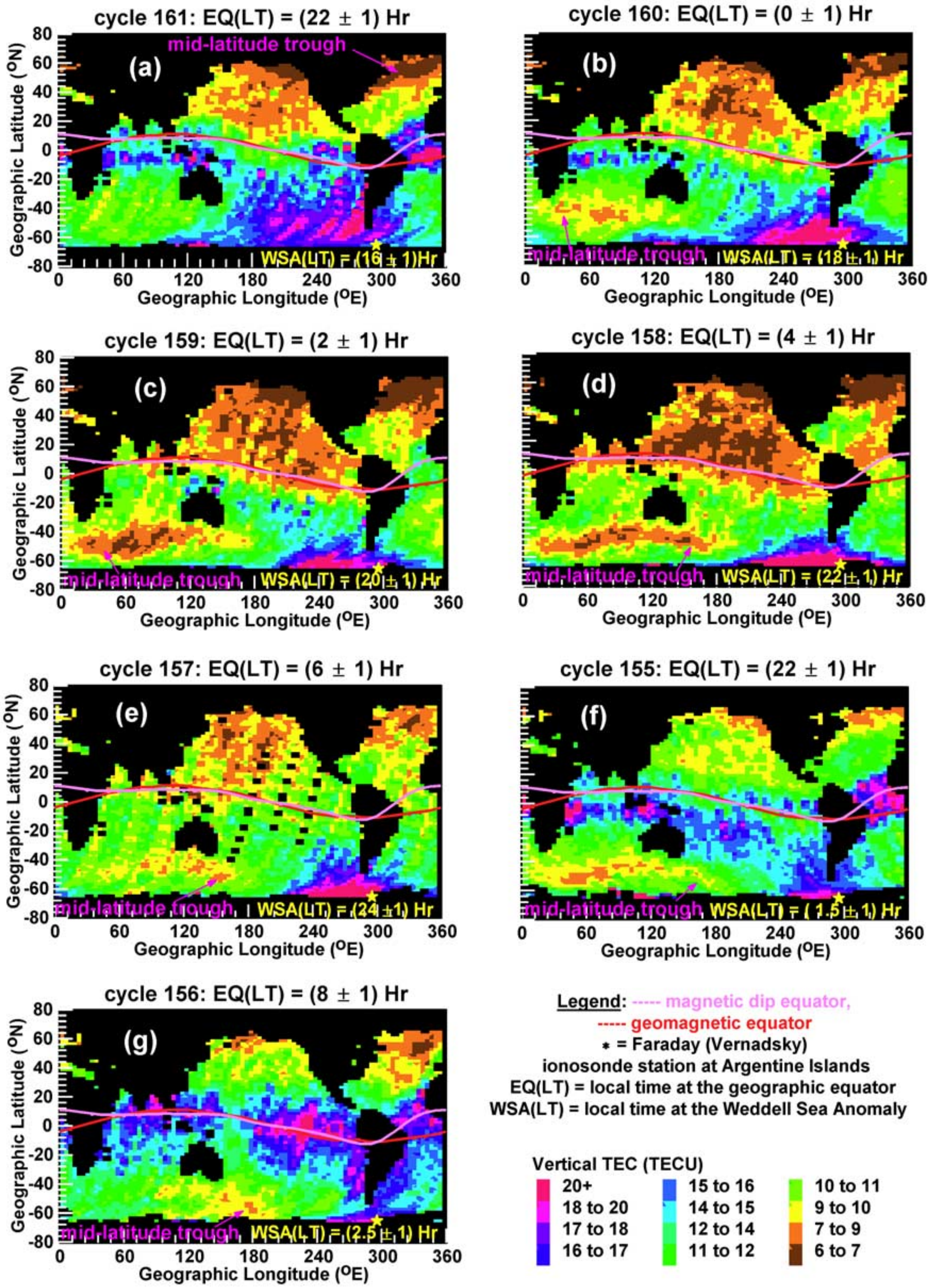

Figure 5. A series of TOPEX TEC maps shows the hourly variations of the nighttime Weddell Sea Anomaly from (16 ± 1) LT to (2.5 ± 1) LT. Regularly, the southern midlatitude trough appears over the Indian, Southern, and southwestern Pacific Oceans; briefly, the northern trough can be seen over the northern Atlantic.

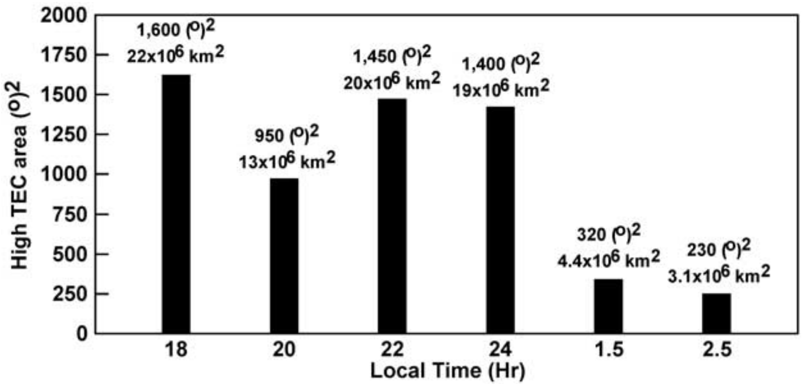

Figure 6. In a histogram form the high TEC areas (computed in latitude degree by longitude degree and in million (10^6) km^2 for a steady ionosphere) are plotted against the LT at 66°S latitude in order to illustrate the hourly variations of the nighttime Weddell Sea Anomaly's area.

equatorward [*Titheridge*, 1995]. First map to indicate its appearance at around 1800 LT over the southeastern Pacific and southwestern Atlantic between 210°E and 300°E (geographic) is shown in Figure 5b. As Figure 5b indicates, the Weddell Sea Anomaly reaches the lowest 45°S geographic latitude at around 260°E and occupies the largest geographical area, estimated as 1600(°)^2 or 22 × 10^6 km^2. At 2000 LT (see Figure 5c), it moves slightly westward and appears between 210°E and 295°E extending up to 55°S at 250°E. Its significantly smaller size, which is around 950(°)^2 or 13 × 10^6 km^2, is apparent (see Figure 5c). At 2200 LT (see Figure 5d) it spreads out in longitudes between 205°E and 325°E and reaches 52°S latitude at 285°E. Its estimated size is the second largest, around 1,450(°)^2 or 20 × 10^6 km^2. At local midnight, when the equatorward neutral winds maximize [*Titheridge*, 1995], the estimated area of Weddell Sea Anomaly remains almost the same (see Figure 5e) that is around 1400(°)^2 or 19 × 10^6 km^2 as before at around 2200 LT. This time its shape is narrower in longitude (210°E–300°E), but wider in latitude reaching 50°S at two longitudes: 250°E and 280°E. After local midnight when the equatorward neutral wind speed rapidly decreases (at around 0300 LT the wind velocity is less than half of its maximum value [*Titheridge*, 1995]), the Weddell Sea Anomaly quickly fades away and probably moves to higher latitudes. At around 0150 LT (see Figure 5f) it occupies a small area of only 320(°)^2 or 4.4 × 10^6 km^2 from 60°S southward and between 240°E and 290°E. This declining process continues after 0200 LT (see Figure 5g), when the Weddell Sea Anomaly appears between 240°E and 285°E at around 65°S latitude over a small area of around 230(°)^2 or 3.1 × 10^6 km^2 at 0250 LT. In form of a histogram, the estimated high TEC areas are plotted against the local time at the Weddell Sea Anomaly (WSA(LT)) in Figure 6. These TOPEX TEC maps and estimated areas (in (°)^2 and million (10^6) km^2) give a clear indication how large in fact the nighttime Weddell Sea Anomaly is. It occupies the higher midlatitude region of the entire southeastern Pacific and southwestern Atlantic. Previous land-based investigations detected only a small section of it over Argentine Islands. With the star symbol, each map in Figure 5 indicates the geographic position of Faraday (now called Vernadsky) ionosonde station at Argentine Islands in South Atlantic Antarctica.

[19] In order to study how the TEC changed in latitude and in local time over the eastern Pacific and western Atlantic Oceans before the development (cycle 161) and soon after the development (cycle 160) of the Weddell Sea Anomaly, and later on during the night (cycle 158), Figure 7 is constructed. Five consecutive odd-numbered passes from 35 to 43, inclusive, from the above mentioned three chosen cycles are plotted in geomagnetic latitude. In these plots, LT values are indicated, as they give a crucial perspective on the data. These TEC line plots are arranged in three columns under the global map of magnetic field lines where the ground tracks of these passes are depicted. At each column the local time (LT) values in decimal hours at the equator (EQ(LT)) and at the Weddell Sea Anomaly (WSA(LT)) are stated. As the magnetic field line configuration is an important driver in the generation of the nighttime Weddell Sea Anomaly, its size and shape are possibly to be dependent upon the magnetic local time (MLT). In order to investigate this MLT dependence, the TEC variations are analyzed in terms of MLT (computed in decimal hours) and geomagnetic latitude. The last plot of each column depicts how the MLT of these passes varies with geomagnetic latitudes in the southern hemisphere for the relevant UT values that are also indicated. At lower geomagnetic latitudes (0°–20°), the magnetic local time remains almost constant. By progressing towards mid and higher magnetic latitudes, the magnetic local time variation shows an increasing trend particularly along passes 35 (approximately 2 hours in MLT over the last 10 degrees (geomagnetic) of the pass) and 037. According to the global field-line map and by progressing from west to east, TOPEX passes 43 and 41 are closer aligned to the magnetic field lines at low and middle latitudes than the other three passes. During the three chosen cycles, passes 43 (~0900 MLT) and 41 (~0800 MLT) detected how the evening midlatitude TEC buildup (shown with passes 43 and 41 of cycle 161) became substantially reduced before local midnight at around 2300 LT (shown with passes 43 and 41 of cycle 160) and after local midnight at around 0300 LT (shown with passes 43 and 41 of cycle 158) over the eastern Pacific. From west to east, TOPEX passes 39 (~0700 MLT), 37 (~0560 MLT), and 35 (~0400 MLT) give latitudinal TEC cross sections of the Weddell Sea Anomaly through its center (see pass 37) situated south of the South American continent that creates a

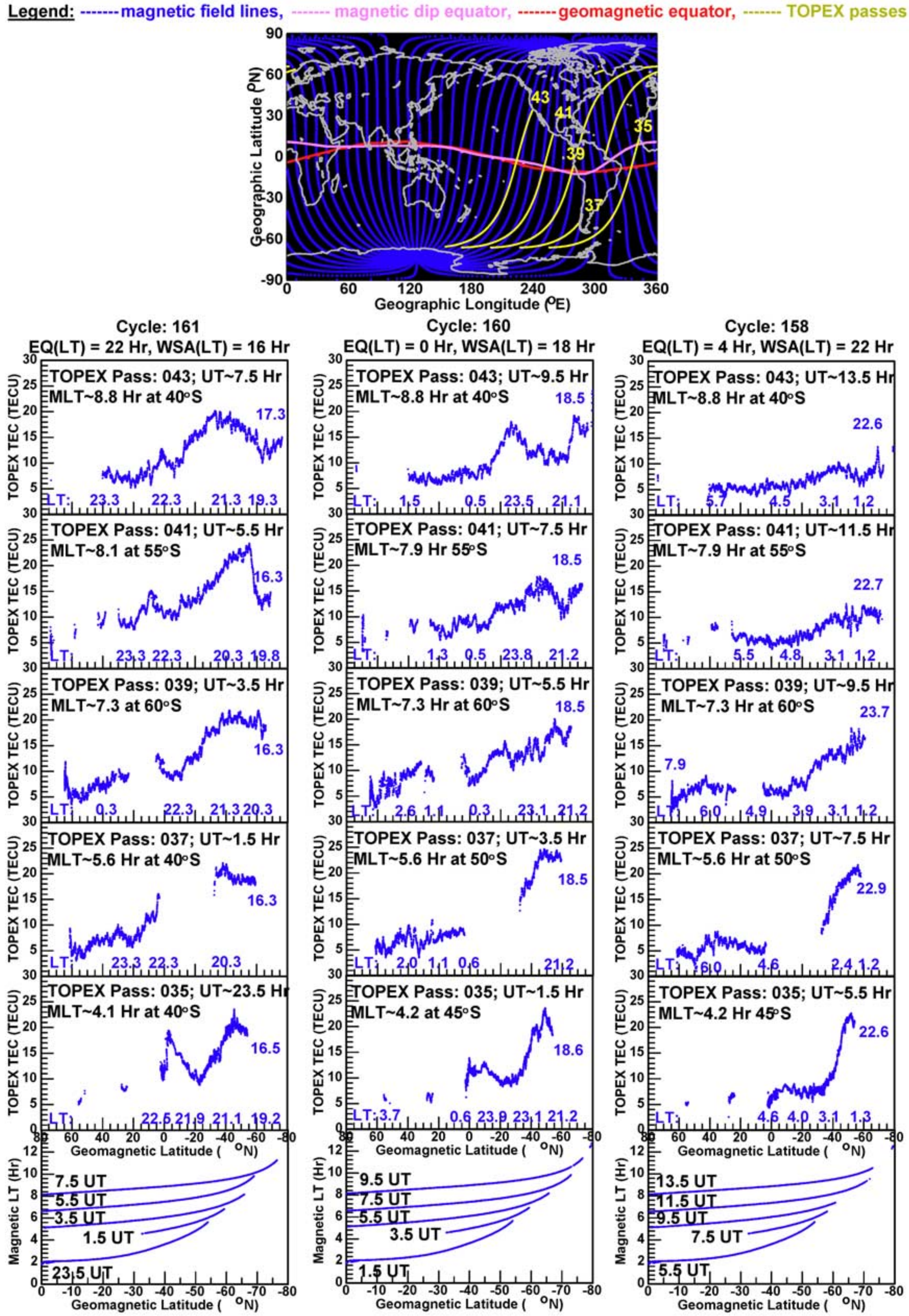

Figure 7. (top) The global map shows the ground tracks of a few passes with the configuration of magnetic field lines. (bottom) Arranged in three columns, the latitudinal TEC line plots from cycles 161, 160, and 158 (from left to right) illustrate the geomagnetic latitudinal (ML) variations of TEC in the region of the Weddell Sea Anomaly. Along the TEC plots, some LT and a certain MLT are also indicated in order to provide some necessary perspective of the data. The bottom row shows MLT variations in southern ML are illustrated for each TOPEX pass.

data gap in that pass as there are no data available over the continents and through its western (see pass 39) and eastern (see pass 35) ends. An interesting feature is the rapidly increasing TEC detected by TOPEX on the equatorward side of the Weddell Sea Anomaly (see pass 035 from cycles 161, 160, and 158). Since the TOPEX data contain mixed spatial and temporal information, differentiating between changes in time (LT or MLT) and changes in latitudes is not possible.

6.2. Winds Effects

[20] Illustrated in Figure 8, a second set of maps is constructed by plotting the magnetic field lines, and a few contour lines of declination angles (D = −10°, 0°, +20°, +30°, +40°) and dip angles (I = 45°S, 55°S) over the TOPEX TEC maps of Figure 5 in order to get an indication where the nighttime Weddell Sea Anomaly appears and how the TEC varies in terms of field line configuration, declination and inclination. From the maps of Figures 8b–8g it becomes obvious that a larger part of the Weddell Sea Anomaly develops over the southeastern Pacific where the spacing between the magnetic field lines is medium, while its smaller eastern edge appears over the southwestern Atlantic, characterized by widely spaced magnetic field lines. In these regions the magnetic midlatitudes are situated at relatively high geographic latitudes (owing to the geographic position of magnetic dip equator), the declination (D) changes from larger positive (+40° or easterly) over the south Pacific through zero to smaller negative (−10° or westerly) over the southwestern Atlantic, and the inclination or dip (I) is close to 55S°. These are all important factors to consider, because as this study's results demonstrate they all affect the spatial distribution of ionospheric plasma. For the Weddell Sea Anomaly region, each factor will be discussed in the next paragraphs.

[21] Owing to its large size, the Weddell Sea Anomaly itself exhibits both a longitudinal and a latitudinal variation. Its development over a wider area of Weddell Sea is due to the significant photoionization taking place throughout the summer nights as the ionosphere remains illuminated between November and February because of the tilted dipole of the Earth [*Sojka et al.*, 1985]. Thus there is plenty of solar produced ionization available for the equatorward directed neutral winds in the magnetic meridional direction (W_m^{mag}) to transport upward along the magnetic field lines to regions of higher altitudes and slower loss. According to current theories [*Rishbeth*, 1972; *Titheridge*, 1995] the sum of true equatorward and eastward geographic components, both are particularly important when the magnetic declination is large, makes up the equatorward component in the magnetic meridional direction:

$$W_m^{mag} = W_m^{geo}\cos D \mp W_Z^{geo}\sin D \tag{7}$$

where

W_m^{mag} = neutral wind in the magnetic meridional direction (+ equatorward),
W_m^{geo} = geographic meridional wind (+ equatorward),
W_Z^{geo} = geographic zonal wind (+ eastward),
D = declination angle (+ eastward),
$\mp$ = northern/southern hemisphere.

[22] Over the southeastern Pacific, the better development of the Weddell Sea Anomaly is partially due to the positive (eastward) and large magnetic declination (D) angles that make the thermospheric neutral winds in the magnetic meridional more effective via the positive contribution from the eastward geographic zonal wind component (W_Z^{geo} sinD) in moving the plasma along the magnetic field lines [*Jee et al.*, 2004, 2005b]. Generally, if D is large (around 45°), then, cosD and sinD are similar (both are around $\sqrt{2}/2$ or 0.7071), and both components become significant [*Bailey et al.*, 2000]. At small or zero declination, the positive contribution from the geographic zonal component is small or no longer available, respectively. To explain this, if D is small (around zero), then cosD ~ 1 and sinD ~ 0. It means that for small declination angles (D ~ 0), the geographic zonal wind component becomes negligible (W_Z^{geo} sinD ~ 0 because sinD ~ 0) and the geographic component alone makes up the magnetic component in the meridional direction ($W_m^{mag} \sim W_m^{geo}$) as cosD ~ 1. In Figures 8b–8c the TEC maps show how the highest TEC values (18+ indicated in light and dark pink) extend up to the 0° declination contour only. Not only locally in the Weddell Sea Anomaly region, but globally as well, the geographic zonal wind as a significant component can introduce a strong longitudinal variation of the spatial distribution of electron density via the longitudinal variations of declination angle [*Rishbeth*, 1972; *Titheridge*, 1995; *Jee et al.*, 2005b]. Global longitudinal TEC variations will be discussed in section 6.5.

[23] Dip angles have a well-known principal role in varying the effectiveness of neutral winds because winds in the magnetic meridional direction (see equation (7)) can be resolved into a field-aligned ($W_{II} = W_M\cos I$) component and a component perpendicular ($W_P = W_M\sin I$) to W_{II}. While the W_{II} component carries ionization along the magnetic field lines with an effective vertical velocity of V' (see equation (8)), the W_P component has no direct effect on the ionization [*Titheridge*, 1995].

$$V' = W_{II}\sin I = W_M\cos I\sin I = 0.5W_M\sin(2I) \tag{8}$$

where

V' = effective vertical wind velocity (+ equatorward),
W_{II} = field aligned component (+ equatorward),
W_M = magnetic meridional component (+ equatorward)

[24] Thus the strength of plasma drift becomes strongest at 45° dip angle (I) [*Khol and King*, 1967; *Dudeney and Piggott*, 1978], and remains large at dip angles between 20°–70° corresponding to dip latitudes of 10°–54° [*Titheridge*, 1995]. During the night, upward ionospheric drifts are produced by the equatorward neutral winds that move the ionization to higher altitudes along the magnetic field lines where the loss rates are lower and thus increase the electron density and TEC. As Figure 8 shows, the effects of dip angle in the spatial distribution of nighttime TEC in the Weddell Sea Anomaly region are obvious. During its best-developed period, at 1800 LT (see Figure 8b), the 45S° (I) contour line clearly marks

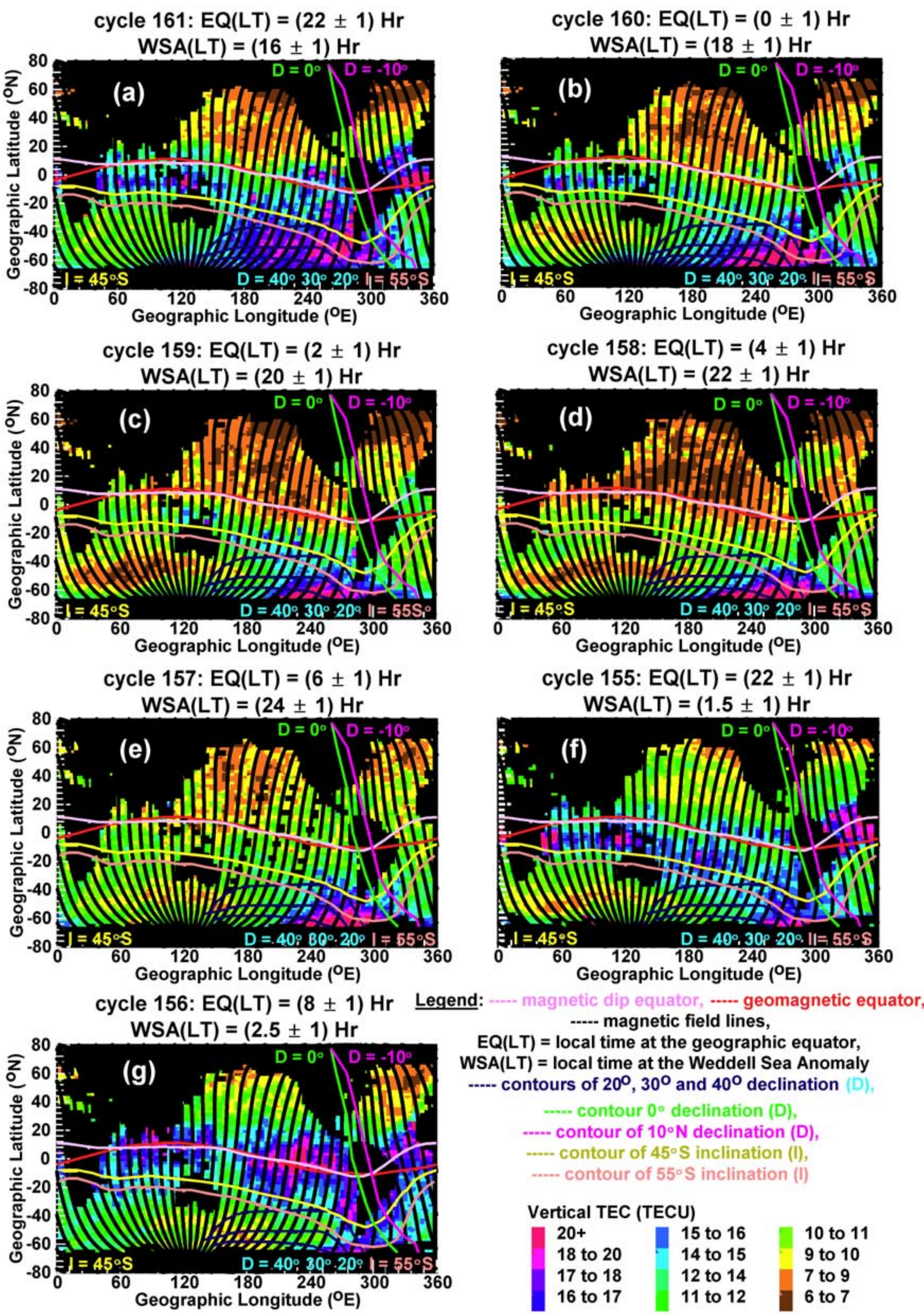

Figure 8. A global field-line map plus a few declination (D: −10°, 0°, 20°, 30°, 40°) and inclination (I: 45°S, 55°S) contours are added to each TOPEX TEC map illustrated in Figure 5 in order to analyze the spatial variations of TEC over the oceans.

the equatorward boundary of the Weddell Sea Anomaly. Later on during the night, when the Weddell Sea Anomaly became less developed, its northern boundary moved to higher latitudes into the position of 55S° (I) contour line.

[25] Considering the configuration of magnetic field lines is important because neutral winds in the magnetic meridional move the plasma along the magnetic field lines. Owing to the significant role of equatorward neutral winds in the development and maintenance of the nighttime Weddell Sea Anomaly, this space weather feature has a natural alignment to the magnetic field lines. This alignment is most obvious over the southeastern Pacific where the winds are more effective and consequently the nighttime TEC values are higher. Figures 8b, 8c, and 8e show very clearly how the western longitudinal boundary of the Weddell Sea Anomaly lies on a certain magnetic field line. High electron densities, extending along a magnetic field line to lower latitudes where the dip angle is around 45°, form its pointy northern edge. Usually, the Weddell Sea Anomaly reaches the lowest geographic latitude at around 45°S dip latitude along the magnetic field line that passes through its center (see further details in section 6.5).

6.3. Electric Fields Effects

[26] At higher middle and at high geomagnetic latitudes, the effective vertical neutral wind component (see equation (8)) is very small, and thus the direct lifting effects of the winds are also very small. As the vertical wind effects disappear at V'∼0, the winds no longer provide a perturbing effect on the ionosphere along the magnetic field lines. However, there is a large interaction between the ionosphere and the neutral atmosphere that creates a large horizontal circulation of the plasma driven by east-west electric fields of magnetospheric origin (**E**) that interact (i.e., form a cross product (**x**)) with the north-south magnetic fields (**B**). This large horizontal circulation produces large-scale convection patterns, which drive the high-latitude winds [*Titheridge*, 1995]. These east-west electric fields transport the ionization primarily perpendicular to the magnetic field lines [*Kendall and Pickering*, 1967; *Anderson*, 1976]. For a conventional convection pattern, wherein the dawn-dusk electric field is situated in the equatorial plane and a stagnation point is at dusk [*Kavanagh et al.*, 1968], several high-latitude ionospheric features can be accounted for. On the nightside due to the westward **E** × **B** drift and normal F region processes [*Knudsen*, 1974; *Quegan et al.*, 1982; *Whalen*, 1989], a midlatitude ionization trough that is well known since the first observations of *Muldrew* [1964] and *Sharp* [1964] can be found equatorward of the auroral zone at around 57° invariant latitude. At F region heights the electron concentration varies the same way as the O^+ concentration. Thus the trough can be observed as a depletion in the electron concentration, which usually implies a depletion in of the O^+ concentration [*Quegan et al.*, 1982]. As a steady ionospheric feature in the nighttime sector, the trough did not get smeared by the data binning procedure of this study, and thus it appeared in both hemispheres during the studied period. Regularly, over the South Indian and Southern Oceans up to the western edge of South Pacific (see Figures 6b–6g), and briefly over the North Atlantic (see Figure 6a). During summer nights, the trough does not develop over the southeastern Pacific and southwestern Atlantic Oceans because the significant production of ionization by solar radiation prevents the formation of a trough [*Rodger and Pinnock*, 1982; *Rodger and Aarons*, 1988]. According to the TEC maps of this study, TOPEX detected the trough in the narrow low-TEC strip (6–7 TECU indicated as dark brown, 7–9 TECU indicated as light brown) showing a strong alignment with the magnetic dip equator.

6.4. Geomagnetic Variations

[27] A set of Kp histograms is prepared and averaged Kp values are computed in order to monitor the level of geophysical disturbance during the period studied (see Figure 4). Kp ∼ 2.15 is the highest average value characterizing the first (cycle 161) and last (cycle 156) TOPEX TEC maps in Figures 5 and 8. Except the 10 January 1997 magnetic storm occurring during cycle 159, the magnetic activity was mostly medium and quiet during the other cycles. Under these magnetic conditions and with the exception of a sudden decrease in area at 2000 LT (cycle 159), the estimated area of the Weddell Sea Anomaly numerically characterizing its state of development (see Figure 6) shows a slightly decreasing trend between 1800 LT and 2400 LT. This trend could reflect the combination of increasing strength of equatorward neutral winds and the decreasing amount of solar produced ionization available as the local time progresses into the night. The strength of winds increases from 0 m/s at 1700 LT when they turn equatorward to 80 m/s at 2400 LT when they reach their maxima [*Titheridge*, 1995].

[28] There is a sudden fall in size of estimated area at 2000 LT (cycle 159) when the Weddell Sea Anomaly becomes 41% smaller than at 1800 LT. This could be explained with the effects of 10 January magnetic storm. Well-known effects of storms on the ionosphere are the positive and negative phases in which the normal TEC largely increases and decreases, respectively, due to the profound changes in the neutral atmospheric composition. Because of the divergent nature of winds, regions of upwelling and downwelling are created leading to the formation of storm phases. Regions of upwelling are rich in nitrogen (N_2) and oxygen (O_2), cause the ionosphere to decay faster than normal and create the negative phases of ionospheric storms. Opposite to these, regions of downwelling are depleted in nitrogen (N_2) and oxygen (O_2), cause the ionosphere to decay more slowly than normal and create the positive phases of ionospheric storms [*Rishbeth*, 1998; *Buonsanto and Fuller-Rowell*, 1997; *Buonsanto*, 1999]. Negative phases are always observed at high latitudes and are more common at midlatitudes than the positive phases [*Jee et al.*, 2004]. Magnetic storms are a form of space weather when the solar wind energy, deposited in the auroral zone, gets dissipated into the ionosphere and thermosphere while various mechanisms and processes become complex. To investigate the response of the Weddell Sea Anomaly to a magnetic storm in detail is beyond the scope of this paper. However, this interesting topic will be the subject of next study and will be reported in another paper.

6.5. Longitudinal Variations

[29] Because of the sensitivity of TEC to the various geophysical factors (such as D, I, B), particularly to the magnetic field-line configuration and declination (both

strongly vary with geographic longitude in the southern hemisphere), there are important longitudinal variations of the southern nighttime ionosphere that are evident in the TEC maps (see Figures 5 and 8). Four very different geographic longitude sectors can be identified according to the nighttime TEC variations. By progressing from west to east in eastern longitudes, these are the Indian, western Pacific, eastern Pacific, and Atlantic longitude sectors. The strong division of Pacific into western and eastern regions is most evident during summer nights. Eastern Pacific is the longitude sector where the conditions are most favorable for creating and maintaining high nighttime electron densities that give rise to the development of the nighttime Weddell Sea Anomaly. This longitude sector was described in detail in the last two paragraphs of section 6.1.

[30] In the longitude sector of the Indian Ocean, conditions are opposite to those of the eastern Pacific. Because of the alignment of geomagnetic and magnetic equators, high geomagnetic and magnetic latitudes are situated at relatively low geographic latitudes. Thus there is no photoionization taking place at night and therefore the TEC is lower. Further, the high dip (I) angles (I $\sim$ 70S°) at geographic midlatitudes make the plasma drift weak via the small sin2(I) component. Declination angles are westward, which indicates that geographic zonal winds transport the ionization down the magnetic field lines to lower altitudes where the loss rates are high. Their opposite effect weakens the equatorward neutral winds [*Titheridge*, 1995; *Jee et al.*, 2005b]. As a net result, equatorward neutral winds become least effective over the Indian Ocean between 40°S and 60°S geographic latitudes, and the levels of ionization are lowest there. At middle geographic latitudes, the TEC is from 50% to 70% less than at the Weddell Sea Anomaly (see Figure 8).

[31] Over the western Pacific longitude region, where the geomagnetic and magnetic dip equators overlap, conditions are intermediate compared with those in the Indian and eastern Pacific regions. Medium geomagnetic and magnetic latitudes are situated at around medium geographic latitudes because of the alignment of overlapping equators. During southern summer nights, there is some photoionization taking place at higher geographic latitudes, as they receive some sunshine. At midlatitudes the dip angles are closer to the optimum value of 55° (than over the Indian Ocean), making the nighttime thermospheric winds more effective in moving the ionization, which is more abundant than over the Indian Ocean but considerably less than over the eastern Pacific, up the magnetic field lines. Eastward directed geographic zonal winds are stronger because of the large eastward (positive) declination angles, and by moving the ionization upward strengthen the equatorward directed neutral winds in the magnetic meridional direction. These geophysical factors create and maintain midlatitude electron densities that are approximately 25%–40% lower than at the Weddell Sea Anomaly, where conditions reach their positive extreme, but up to 50% higher than over the Indian Ocean where conditions are least favorable.

[32] Over the South Atlantic, some conditions are similar but others are different than that in the eastern Pacific longitude sector. Close to the South American continent, middle geomagnetic latitudes are still situated at high geographic latitudes because of the geographic position of geomagnetic equator and the dip angles are still in the optimum range of 10°–70° (I $\sim$ 55S°; see Figure 8). These correspondingly mean that there is still plenty of photoionization taking place during summer nights and the equatorward directed thermospheric neutral winds in the magnetic meridional direction are still strong enough to move effectively the ionization up the magnetic field lines. However, the declination angle is westward (negative) indicating that the geographic zonal winds do not contribute to but oppose the geographic meridional winds, and therefore the net effect of thermospheric neutral winds in the meridional direction is less than in the eastern Pacific longitude region. As a result of the above explained geophysical conditions over the South Atlantic, the Weddell Sea Anomaly develops in a better form over the southwestern Atlantic region and close to the South American continent.

[33] Figure 9 is constructed with a series of TEC and declination (D) line plots to further investigate the longitudinal variations of TEC in terms of D. Longitudinal TEC cross sections along northern 40°, plus southern 40°, 50°, 60°, and 66° geographic latitudes are prepared with averaged TEC values from the same cycles (i.e., 161, 160, and 158) that were utilized for Figure 7. During these cycles TOPEX detected the ionosphere before the development (cycle 161) and soon after the development (cycle 160) of the Weddell Sea Anomaly, and later on during the night (cycle 158). On the top of Figure 9 there is a global magnetic field-line map where the geographic position of each longitudinal TEC section is mapped in order to view them with the magnetic field lines. In three columns, one for each chosen cycle, a series of longitudinal TEC cross sections along the designated latitudes are plotted with the declination angles. Local time values are also indicated in each graph. In the southern hemisphere these TEC cross sections cut across the Weddell Sea Anomaly close to its northern (40°S) and southern (60°S and 66°S) ends and at around its middle section (50°S). There is a strong correlation between the variations of TEC and declination along latitudes 40°S, 50°S, and 60°S during these three cycles. Particularly during cycle 161 along 40°S latitude, at 2090 LT, where the TEC and D variations are most similar. These TEC and D variations cannot be compared directly because of their different units. In many graphs of cycle 160 the average TEC and D curves overlap, which is due to the scale used on the graph only. Particularly at latitudes 60°S and 66°S, the large positive values of D over the Pacific Ocean (between 150°E and 300°E) suddenly turn negative at around 120°E and remain negative over the Indian and Atlantic Oceans. Along 66°S latitude, where the TOPEX/Poseidon satellite turns, the TEC profile at 2220 LT (cycle 158) shows high TEC values over the southeastern Pacific (between 240°E and 300°E longitude) giving a clear indication that the Weddell Sea Anomaly continues at higher latitudes. These TEC and D line plots demonstrate how dominating is the declination effect and how strongly the declination angle varies with longitude in the southern hemisphere.

[34] Along the 40°N geographic latitude in the sectors of Indian and Pacific, the declination angles are small and positive, and their variations are little. D turns negative at around 250°E, and there are slightly larger (but still small compared with the southern hemisphere) variations of

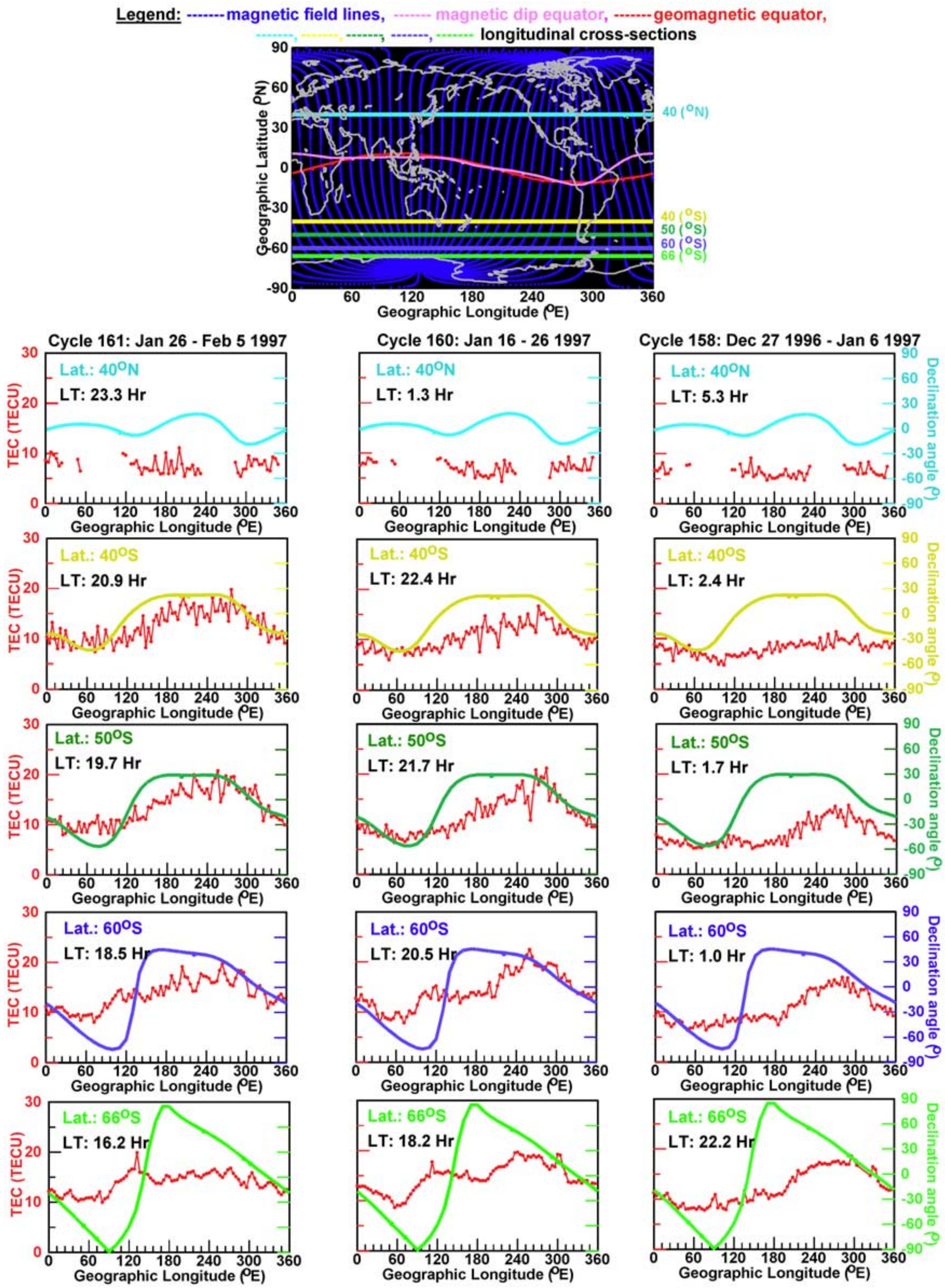

Figure 9. (top) The global map shows the ground tracks of longitudinal TEC cross sections along one northern (40°N) and a few southern (40°S, 50°S, 60°S, and 66°S) latitudes with the magnetic field lines. (bottom) Arranged in three columns, the longitudinal TEC cross sections from cycles 161, 160, and 158 illustrate the longitudinal variations of TEC and declination (D) along the selected latitudes.

negative D over the Atlantic Ocean. The corresponding latitudinal TEC profile follows quite closely the weak longitudinal dependence of declination angle. Because of the small magnetic declination in the northern hemisphere, contributions from the geographic zonal winds to the neutral winds in the meridional direction are negligible. As a result, the magnetic meridional winds approach the geographic meridional winds. This excludes any significant longitudinal variations of F region electron density. Thus the relatively small longitudinal variations of TEC in the northern hemisphere are due to the small declination variations [*Jee et al.*, 2004, 2005b].

6.6. Summer-Winter Variations

[35] Almost 3 months of data are presented in the form of nighttime TOPEX TEC maps that are suitable for investigating summer-winter variations between the two hemispheres as they combine northern winter with southern summer. Since the data coverage is considerably less in the northern hemisphere because of the large land masses of continents, only the Pacific and Atlantic longitude sectors are possible to investigate. When inspecting the TOPEX TEC maps of Figure 5, the most striking features in the northern hemisphere winter nighttime TEC pattern are the low TEC and the lack of longitudinal variations. Winter nighttime TEC values at middle (around 40°N; see Figure 9) and higher (around 60°N) geographic latitudes are lowest, approximately 6–9 TECU (indicated as dark and light brown), particularly over the Northern Pacific. Observed also by *Jee at al.* [2004], the winter-summer combination creates a TEC pattern that is highly asymmetric about the magnetic equator. Particularly, the first five TEC maps (from Figure 5a to Figure 5e) show this strong asymmetry where the northern hemisphere is still in nighttime darkness before local sunrise. Higher TEC levels in the northern hemisphere are evident in the last three maps constructed with cycles 157, 155, and 156 and are due to the later local times. Cycle 157 shows the northern hemisphere after local sunrise. Cycle 155 shows the northern ionosphere in the evening sector between 1800 LT (at 66°N) and 2200 LT (EQ(LT)), while also an early morning (0800 LT at the equator) to late morning (1100 LT at 66°N) northern ionosphere is imaged by cycle 156.

7. Summary and Conclusion

[36] In the first part of this paper a short review of the TOPEX/Poseidon mission and technique was given, the TEC theory relevant for this technique was explained and a custom-made software package developed for obtaining numerical TEC values (in TECU) from the raw TOPEX radar data was introduced. Experimental aspects of the TOPEX/Poseidon technique, of which understanding is important for analyzing observational results, were described and demonstrated.

[37] In the second part, the nighttime space weather variations of the low sunspot number (F10.7∼90) 1996/1997 southern summer were investigated by the space-based TOPEX/Poseidon radar technique. Over-the-ocean TOPEX TEC data collected for the period of 28 November 1996 to 5 February 1997 were utilized to create a series of seven nighttime TEC maps and several latitudinal and longitudinal TEC line plots. These observational results were combined with global magnetic field-line maps and with line plots of declination data in order to ascertain the morphology of the spatial TEC distribution over the oceans.

[38] According to the nighttime TOPEX TEC map series, the most outstanding feature of the nighttime ionosphere is the nighttime Weddell Sea Anomaly. Appearing as a prominent nighttime ionization enhancement over the southeastern Pacific and southwestern Atlantic Oceans, it is a large ionospheric space weather feature. Over 4 hours of LT and 2 hours of MLT, a rapid TEC increase in latitudes toward the source of photoionization that is the solar illuminated high-latitude region, characterizes its image detected by the onboard NRA. In longitudes, its TEC cross section is a broad buildup extending from around 200°E (geographic) sometimes up to 320°E, while the nighttime TEC peaks at around 250°E–270°E and between 50°S and 60°S. Owing to its regular appearance on the TEC maps, it was possible to investigate its hourly variations. Under the assumption that the nighttime Weddell Sea Anomaly did not change significantly during the approximately 4 hour LT variation introduced by the TOPEX TEC data, its size was estimated in $(°)^2$ and million (10^6) km^2 for comparative purposes only. Its hourly variations were compared with the published [*Titheridge*, 1995] neutral wind speed values. According to observational results, the Weddell Sea Anomaly appeared first at around 1800 LT, soon after the neutral winds turned equatorward (around 1700 LT). At its best stage of development (1800 LT), it appeared over a geographic area of $1600(°)^2$ or 22×10^6 km^2 and remained well developed ($\sim 1400(°)^2$; $\sim 19 \times 10^6$ km^2) until local midnight that is the time when the equatorward neutral wind speed in the magnetic meridional direction maximizes. After 0000 LT, it faded away suddenly ($320(°)^2$ or 4.4×10^6 km^2 and $230(°)^2$ or 3.1×10^6 km^2) and simultaneously with the rapid decline of above mentioned neutral wind speed. During the 10 January 1997 magnetic storm there was a sudden 43% decrease in area possibly caused by the negative storm effects. To investigate storm effects in detail is beyond the scope of this paper and will be the subject of next study. Because of the binning procedure applied by other researchers, both the daytime and nighttime phenomenon of the Weddell Sea Anomaly remained undetected by the global TOPEX TEC maps of previous space climate studies published in the literature.

[39] In the southern hemisphere a strong correlation has been found between the longitudinal variations of nighttime TEC imaged by the TOPEX maps and declination leading to the identification of four longitudinal sections. Namely these are the Indian, western Pacific, eastern Pacific, and Atlantic regions. While previous climatology studies recognized three longitudinal sectors only, the presence of nighttime Weddell Sea Anomaly that strongly divides the Pacific Ocean into western and eastern regions warranted a division of four. Into this longitudinal division of four, the global field-line configuration pattern that also varies with longitudes in terms of line spacing and orientation fits perfectly. Global field-line maps plotted over the TOPEX TEC maps provided clear evidence. Indication has also been found and presented that the nighttime Weddell Sea Anomaly develops

where the spacing between the magnetic field lines are medium/large, and where medium geomagnetic/m latitudes are situated at relatively high geographic latitudes due to the geographic position of overlapping geomagnetic/magnetic dip equators creating a large 12° offset in the southern hemisphere with respect to the geographic equator.

[40] Although earlier work of *Horvath and Essex* [2003] investigated the 1998/1999 southern summer period, and the space science community has covered the nighttime Weddell Sea Anomaly and the associated research topics, this study is considered significant because of its new findings that do move science forward. These new findings are as follows:

[41] 1. The center of nighttime Weddell Sea Anomaly during the 1996/1997 summer appeared at around 50°S–60°S and 250°E–270°E geographic coordinates.

[42] 2. This study's preliminary investigations have revealed that the 10 January 1997 magnetic storm had a significant (43%) reducing effect, possibly caused by the negative storm effects, on the measurable average area of the nighttime Weddell Sea Anomaly.

[43] 3. Evidence presented in the form of longitudinal TEC cross sections has confirmed that the nighttime Weddell Sea Anomaly continues at latitudes higher than 66°S where TOPEX TEC data coverage is not available because of the 66° inclined satellite orbit.

[44] 4. Through a novel geographical presentation obtained by adding the 45°S and 55°S inclination (I) plus some declination (D) contours to the combined TOPEX TEC and magnetic field-line maps for the first time, the principal role of thermospheric neutral winds in changing TEC was highlighted.

[45] 5. Longitudinal TEC cross sections, placed between 40°S and 66°S mostly at approximately 10 degree intervals and cutting across the Weddell Sea Anomaly, have revealed that there is link between longitudinal variations of TEC and declination in the region of nighttime Weddell Sea Anomaly. These sorts of longitudinal investigations of the Weddell Sea Anomaly have never been carried out and reported in the literature before.

[46] In conclusion this study has provided several interesting new results, summarized and listed above, on the nighttime Weddell Sea Anomaly. Developing over a considerable geographic area (around $1600(°)^2$ or 22 million km^2 computed for a steady ionosphere) during the southern 1996/1997 summer, the nighttime Weddell Sea Anomaly is a large space weather feature of the nighttime southern ionosphere. Its image remained undetected by the global TOPEX TEC maps of previously published climate studies of other researchers because of the smearing effect of their binning procedure and remained overlooked even when its ionospheric signature appeared on their line plots. It is believed that the new findings reported in this paper will increase current knowledge and understanding of this space weather feature, which is basically still unknown by the larger science community.

[47] **Acknowledgments.** Ildiko Horvath is supported by a University of Queensland Postdoctoral Research Fellowship. Special thanks are extended to NOAA's Geophysical Data Centre for the geomagnetic data and to JPL for the TOPEX radar data. The TOPEX data were obtained from the NASA Physical Oceanography Distributed Active Archive Centre and the Jet Propulsion Laboratory/California Institute of Technology.

[48] Zuyin Pu thanks Martin Jarvis and another reviewer for their assistance in evaluating this paper.

References

Anderson, D. N. (1976), Modeling the midlatitude F-region ionospheric storm using east-west drift and meridional wind, *Planet. Space Sci.*, *24*, 69–77.

Bailey, G. J., M. H. Denton, R. A. Heelis, and S. Venkatraman (2000), A modelling study of the latitudinal variations in the nighttime plasma temperatures of the equatorial topside ionosphere during northern winter at solar maximum, *Ann. Geophys.*, *18*, 1435–1446.

Bellchambers, W. H., and W. R. Piggott (1958), Ionospheric measurements made at Halley Bay, *Nature*, *188*, 1596–1597.

Buonsanto, M. J. (1999), Ionospheric storms – A review, *Space Sci. Rev.*, *88*, 563–601.

Buonsanto, M. J., and T. J. Fuller-Rowell (1997), Strides made in understanding space weather at Earth, *Eos Trans. AGU*, *78*, 1–7.

Clilverd, M. A., A. J. Smith, and N. R. Thomson (1991), The annual variation in quiet time plasmaspheric electron density, determined from whistler mode group delays, *Planet. Space Sci.*, *39*, 1059–1067.

Codrescu, M. V., S. E. Palo, X. Zhang, T. J. Fuller-Rowell, and C. Poppe (1999), TEC climatology derived from TOPEX/POSEIDON measurements, *J. Atmos. Sol. Terr. Phys.*, *61*, 281–298.

Codrescu, M. V., K. L. Beierle, T. J. Fuller-Rowell, S. E. Palo, and X. Zhang (2001), More total electron content climatology from TOPEX/Poseidon measurements, *Radio Sci.*, *36*, 325–333.

Dudeney, J. R., and W. R. Piggott (1978), Antarctic ionospheric research, in *Upper Atmospheric Research in Antarctica*, *Ant. Res. Ser.*, vol. 29, edited by L. J. Lanzerotti and C. G. Park, pp. 200–235, AGU, Washington, D. C.

Fu, L. L., E. J. Christensen, C. A. Yamarone Jr., M. Lefebvre, Y. Menard, M. Dorrer, and P. Escudier (1994), TOPEX/POSEIDON mission overview, *J. Geophys. Res.*, *99*, 24,369–24,381.

Horvath, I., and E. A. Essex (2003), The Weddell Sea Anomaly observed with the TOPEX satellite data, *J. Atmos. Sol. Terr. Phys.*, *65*, 693–706.

Jee, G., R. W. Schunk, and L. Scherliess (2004), Analysis of TEC data from the TOPEX/Poseidon mission, *J. Geophys. Res.*, *109*, A01301, doi:10.1029/2003JA010058.

Jee, G., R. W. Schunk, and L. Scherliess (2005a), Comparison of IRI-2001 with TOPEX measurements, *J. Atmos. Sol. Terr. Phys.*, *67*, 365–380.

Jee, G., R. W. Schunk, and L. Scherliess (2005b), On the sensitivity of total electron content (TEC) to upper atmospheric/ionospheric parameters, *J. Atmos. Sol. Terr. Phys.*, *67*, 1040–1052.

Kavanagh, L. D., Jr., J. W. Freeman Jr., and A. J. Chen (1968), Plasma flow in the magnetosphere, *J. Geophys. Res.*, *73*, 5511–5519.

Kendall, P. C., and W. M. Pickering (1967), Magnetoplasma diffusion at F2 regions altitudes, *Planet. Space Sci.*, *15*, 825–833.

Khol, H., and J. W. King (1967), Atmospheric winds between 100 and 700 km and their effects on the ionosphere, *J. Atmos. Terr. Phys.*, *29*, 1045–1062.

Knudsen, W. C. (1974), Magnetospheric convection and the high-latitude F2 ionosphere, *J. Geophys. Res.*, *79*, 1046–1055.

Menard, Y., M. Lefebvre, P. Escudier, and L. Fu (1995), Ocean and climate: A quantitative answer, TOPEX/POSEIDON, *Acta Astron.*, *37*, 293–299.

Monaldo, F. (1993), TOPEX ionospheric height correction precision estimated from prelaunch test results, *IEEE Trans. Geosci. Remote Sens.*, *31*(2), 371–375.

Muldrew, D. B. (1964), F-Layer ionization trough deducted from Alouette data, *J. Geophys. Res.*, *70*, 2635–2650.

Penndorft, R. (1965), The average ionospheric conditions over the Antarctic, in *Geomagnetism and Aeronomy*, *Ant. Res. Ser.*, vol. 4, edited by A. H. Waynick, pp.1–45, AGU, Washington, D. C.

Quegan, S., G. J. Bailey, R. J. Moffett, R. A. Heelis, T. J. Fuller-Rowell, D. Rees, and R. W. Spiro (1982), Theoretical study of the distribution of ionization in the high-latitude ionosphere and the plasmasphere: First results on the mid-latitude trough and the light-ion trough, *J. Atmos. Terr. Phys.*, *44*, 619–640.

Rishbeth, H. (1972), Thermospheric winds and the F region: A review, *J. Atmos. Terr. Phys.*, *34*, 1–47.

Rishbeth, H. (1986), On the F2-layer continuity equation, *J. Atmos. Terr. Phys.*, *48*, 511–519.

Rishbeth, H. (1998), How the thermospheric circulation affects the ionospheric F2-layer, *J. Atmos. Sol. Terr. Phys.*, *60*, 1385–1402.

Robinson, T. R., and R. Beard (1995), A comparison between electron content deduced from the IRI and that measured by the TOPEX duel frequency altimeter, *Adv. Space Res.*, *16*, 155–158.

Rodger, A. S., and J. Aarons (1988), Studies of ionospheric F-region irregularities from geomagnetic mid-latitude conjugate regions, *J. Atmos. Sol. Terr. Phys.*, *50*, 63–72.

Rodger, A. S., and M. Pinnock (1982), Movements of the mid-latitude ionospheric trough, *J. Atmos. Sol. Terr. Phys.*, *44*, 985–992.

Sharp, G. W. (1964), Mid latitude trough in the nighttime ionosphere, *J. Geophys. Res.*, *81*, 3156–3271.

Sojka, J. J., W. J. Raitt, R. W. Schunk, and J. L. Parish (1985), Diurnal variations of the dayside, ionospheric, mid-latitude trough in the southern hemisphere at 800 km: Model and measurement comparison, *Planet. Space Sci.*, *33*, 1375–1382.

Titheridge, J. E. (1995), Winds in the ionosphere–A review, *J. Atmos. Terr. Phys.*, *57*, 1681–1714.

Whalen, J. A. (1989), The daytime F layer trough and its relation to the ionospheric-magnetospheric convection, *J. Geophys. Res.*, *94*, 17,169–117,184.

I. Horvath, Electromagnetics and Imaging, School of Information Technology and Electronic Engineering, University of Queensland, St. Lucia, Brisbane, QLD, 4072, Australia. (ihorvath@itee.uq.edu.au)